Published in final edited form as:

Nature. 2010 August 12; 466(7308): 887–890. doi:10.1038/nature09192.

Dynamics and Mechanism of Repair of UV-induced (6-4) Photoproduct by Photolyase

Jiang Li[1], **Zheyun Liu**[1], **Chuang Tan**[1], **Xunmin Guo**[1], **Lijuan Wang**[1], **Aziz Sancar**[2], and **Dongping Zhong**[1,†]

[1]Departments of Physics, Chemistry, and Biochemistry, Programs of Biophysics, Chemical Physics, and Biochemistry, 191 West Woodruff Avenue, The Ohio State University, Columbus, OH 43210.

[2]Department of Biochemistry and Biophysics, University of North Carolina School of Medicine, Chapel Hill, North Carolina 27599.

Abstract

One of the detrimental effects of UV radiation on DNA is the formation of the (6-4) photoproduct (6-4PP) between two adjacent pyrimidines1. This lesion interferes with replication and transcription and may result in mutation and cell death2. In many organisms a flavoenzyme called photolyase uses blue light energy to repair the 6-4PP3. The molecular mechanism of the repair reaction is poorly understood. Here, we use ultrafast spectroscopy to show that the key step in the repair photocycle is a cyclic proton transfer between the enzyme and the substrate. By femtosecond synchronization of the enzymatic dynamics with the repair function, we followed the function evolution and observed direct electron transfer from the excited flavin cofactor to the 6-4PP in 225 ps but surprisingly fast back electron transfer in 50 ps without repair. Strikingly, we found that the catalytic proton transfer between a histidine residue in the active site and the 6-4PP, induced by the initial photoinduced electron transfer from the excited flavin cofactor to 6-4PP, occurs in 425 ps and leads to 6-4PP repair in tens of nanoseconds. These key dynamics define the repair photocycle and explain the underlying molecular mechanism of the enzyme's modest efficiency.

The (6-4) photolyase contains a fully reduced flavin adenine dinucleotide ($FADH^-$) as the catalytic cofactor (Figs 1 and 2a)4–6. Upon excitation the flavin cofactor donates an electron to the 6-4PP to generate a charge-separated radical pair ($FADH^{\bullet}$+6-4PP$^{\bullet-}$)6–8. However, because the formation of 6-4PP involves C6-C4 bond formation and –OH group transfer from the C4 of the 3' pyrimidine to the C5 of the 5' pyrimidine, the direct C6-C4 bond

---

†Correspondence and requests for materials should be addressed to D.Z. dongping@mps.ohio-state.edu. Phone: (614) 292-3044. Fax: (614) 292-7557.

Full Methods and any associated references are available in the online version of the paper at www.nature.com/nature.

Supplementary Information is linked to the online version of the paper at www.nature.com/nature.

Author Contributions D.Z. designed the research. J.L., Z.L., C.T., X.G. and L.W. performed the research. J.L., Z.L., C.T. and D.Z. analyzed the data. J.L., Z.L., A.S. and D.Z. wrote the paper. All authors discussed and edited the manuscript.

Author Information Reprints and permissions information is available at www.nature.com/reprints.

splitting in 6-4PP$^{\bullet-}$ unaccompanied by –OH transfer would simply produce two damaged bases (Fig. 1). Remarkably, (6-4) photolyase catalyzes this complex chemical reaction with no measurable error. Various hypothetical repair models6,9–15, including formation of an oxetane intermediate before the photochemical reaction9,10 and, more recently, a model that includes H_2O formation following the primary photochemical reaction6,11, were proposed to rationalize the bond breakages and group arrangements necessary for repair. Most models invoke proton transfer (PT)5,9,16 from a neighboring histidine residue, leading to a plausible scheme (Fig. 1).

To identify the reaction intermediates and test the proposed repair models we performed ultrafast spectroscopy. We first characterized the initial electron transfer (ET) by analyses of the excited FADH$^-$ dynamics using femtosecond fluorescence spectroscopy7. Monitoring the weak FADH^{-*} emission at 550 nm (Fig. 2a), we found that the fluorescence of FADH^{-*} in the absence of substrate is 3 ns but becomes drastically shorter in the enzyme-substrate complex (Fig. 2b). The transient in the complex can be best represented by a stretched-single-exponential decay, $Ae^{-(t/\tau)\beta}$, with τ=225 ps and β=0.8, reflecting a heterogeneous ET dynamics7,17 that is continuously modulated by the active-site solvation as has been reported recently for (6-4) photolyase18 and as is also observed in photosynthesis19. These results were confirmed by transient absorption spectroscopy of the excited-state flavin dynamics (λ_{pr}=800 nm) (Fig. 2b). Importantly, when the potential active-site proton donor10, His364, was replaced by charged (K and D), polar (N and Y) and hydrophobic (A and M) residues, we observed similar ET dynamics that follow a stretched-single-exponential decay with τ=147-281 ps and β=0.8-0.9 (Supplementary Fig. 1 and Table 1). This finding, along with the observation that the 6-4PP appears to be in its standard form in enzyme-complex X-ray structure6, excludes the early repair model9,10 that requires an oxetane precursor before the photochemical excitation. We conclude that after one electron injection, 6-4PP repair takes place completely in the anionic ground state of 6-4PP$^{\bullet-}$.

After the photoinduced charge separation (FADH$^{\bullet}$+6-4PP$^{\bullet-}$), the reaction can evolve along two pathways, back ET (k_2) or 6-4PP repair (k_3) (Fig. 1). Knowing the forward ET dynamics of FADH^{-*}, we can map out the temporal evolution of FADH$^{\bullet}$ by probing at wavelengths from 500 to 700 nm (Fig. 2a) to follow 6-4PP repair. Clearly, the transient probed at 640 nm (Fig. 2c, red curve) shows a drastically different behavior from that probed at 800 nm (blue curve) due to the capture of the radical FADH$^{\bullet}$ (green curve). Strikingly, we observed an apparent rise signal of FADH$^{\bullet}$ in 45 ps (initial flat part of Fig. 2c inset) and a remarkably long plateau, indicating that complete 6-4PP repair takes longer than several nanoseconds. Because forward ET takes about 225 ps, the 45 ps is the overall decay time of the initially formed FADH$^{\bullet}$ ($(k_2+k_3)^{-1}$ in Fig. 1 and dashed purple curve in Fig. 2c) but appears an apparent rise. Such slower formation and faster decay result in reverse kinetics appearance and less FADH$^{\bullet}$ accumulation. The dynamics of the branched FADH$^{\bullet}$ in the repair channel (Fig. 1 and dashed cyan curve in Fig. 2c) exhibits a complex formation (largely determined by the k_1 process) and a slow decay (k_4) but its amplitude is mainly determined by the k_3 (proton transfer) rate. By deconvolution (Supplementary Information), we obtained back ET in 50 ps (k_2^{-1}) and repair in 425 ps (k_3^{-1}) to form a 6-4PP$^{\bullet-}$ anionic intermediate. From these rate constants we obtained a repair branching of 0.097, a value which is in excellent

agreement with the reported steady-state repair quantum yield of ~0.120, suggesting that after the k_3 step, all subsequent reaction steps proceed to the final 6-4PP repair without any back ET that would lead to a futile cycle. When the probe is tuned to any other wavelengths in the range of 640-500 nm, all resulting transients gave the same dynamics of $FADH^{\bullet}$. These findings reveal that the underlying molecular mechanism for the low repair quantum yield of (6-4) photolyase (~0.1) compared to CPD photolyase (~0.9)4,7 is the fast rate of back ET (k_2^{-1}=50 ps) from $6\text{-}4PP^{\bullet-}$ to $FADH^{\bullet}$ relative to the rate of proton transfer to $6\text{-}4PP^{\bullet-}$ (k_3^{-1}=425 ps), which is an essential step in catalysis.

For the series of mutants (H364N/M/Y/A/D/K) used to test the proposed reaction mechanism, we surprisingly observed that all transients probed in the 500-700 nm region show the similar back ET dynamics in the range of 70-260 ps (Supplemental Table 1 and Fig. 2) but decay to zero without any long plateaus (shown in Fig. 2d for the H364N mutant). This observation is critical to the proposed reaction scheme as it indicates that in the mutants even though ET from $FADH^{-*}$ to 6-4PP is essentially normal, the repair channel is completely shut off and all $FADH^{\bullet}$ formed by initial charge separation follows a futile cycle back to $FADH^{-}$ by charge recombination (Fig. 1). These results are also consistent with our steady-state quantum yield measurements which revealed a total lack of repair with any of the mutants (inset in Fig. 2d). Collectively, our data, in agreement with an earlier report10, indicate that H364 in the active site is a functional residue which is irreplaceable in the repair channel, and proton transfer from H364 to $6\text{-}4PP^{\bullet-}$ is conceivably the rate-limiting step (k_3) in our reaction scheme (Fig. 1).

To test for proton transfer from H364 during the repair reaction, the reaction was carried out in D_2O. As shown in Fig. 2d for wild-type photolyase, we observed a different transient with an obviously lower plateau, reflecting a slower repair process in 1100 ps but with similar forward (212 ps) and back (60 ps) ET dynamics as in H_2O (Supplementary Table 1 and Supplemental Information). Thus, with the deuterated H364, the repair through D^+ transfer slows down by a factor of more than 2. Such a ratio of the rates (k_H/k_D ~2.6) indicates no significant quantum tunneling effect21 for PT in photolyase. The X-ray structure shows a H-bond distance of 2.7 Å between the -NH of H364 and the -OH at the C5 position of the 5' base (Fig. 1); hence, proton transfer from H364 to the –OH is quite feasible. The lower plateau in the transient in D_2O is about a half of that in H_2O (Fig. 2d) and thus corresponds to a half decrease in the repair branching, in good agreement with the steady-state measured quantum yield ratio of 1:2 for D_2O to H_2O (Fig. 2d inset). We also studied both the repair dynamics and the steady-state enzyme activity over a pH range of 7 to 9 and did not note any changes, consistent with the observation that H364 remains protonated over even a wide basic pH range16. All these results are consistent with proton transfer from H364 to $6\text{-}4PP^{\bullet-}$ to generate a protonated neutral radical $6\text{-}4PPH^{\bullet}$, as a key step in the repair pathway (Fig. 1). This critical proton transfer, facilitated by the initial photoinduced electron transfer, completely blocks the futile back ET from $6\text{-}4PP^{\bullet-}$ and allows the reaction to proceed to repair with 100% efficiency after this step.

To further confirm the proposed model, we examined the repair processes by detection of the 6-4PP-related species and the recovery of $FADH^{-}$ in the UV region. Typical transients are shown in Fig. 3; they represent superposition of all species absorbing in UV. Because the

H364N mutant exhibits no repair and only follows a futile forward and back ET cycle by comparing the transients of the wild-type enzyme with those of the H364N mutant we were able to determine the absorption spectrum of $FADH^{-*}$ over the near UV-visible range (Fig. 2a). Knowing the absorption spectra of 6-4PP and of flavins in various forms ($FADH^{-}$, $FADH^{-*}$ and $FADH^{\bullet}$) and their related dynamics obtained by visible-light probing presented above, we obtained the transient dynamics of the 6-4PP intermediate (Fig. 3a,b) formed in about 425 ps with protonated and in about 1100 ps with deuterated H364 and determined its absorption coefficient with a peak around 325 nm (Fig. 2a) (Supplemental Information). Thus, in this system we are able to detect the repair reaction intermediates of both the cofactor ($FADH^{\bullet}$) and the substrate (6-4PP$H^{\bullet}$). After protonation, the substrate intermediate radical decays in nanoseconds, corresponding to a series of atom arrangements with bond breaking and formation to complete the 6-4PP repair on a timescale of tens of nanoseconds.

Based on these findings and previous data, including the crystal structure of the enzyme-substrate complex6, we can propose a catalytic photocycle for the repair of thymine (6-4) photoproduct (Fig. 4). In this scheme, the primary reactions are the initial electron transfer (I to II) and the subsequent proton transfers (II to III). The ET-induced PT from a His residue in photolyase to the 6-4PP is a key step in the repair photocycle, like the “dividing line” in the transition state and making the subsequent reactions “downhill” without the possibility of back reaction. This critical step competes with the back ET resulting in an overall repair quantum yield of about 0.1, which is probably the maximum value that could be achieved for such a structurally and chemically challenging reaction, through slowing down back ET and speeding up the PT processes. The successive elementary steps naturally proceed to an intramolecular PT from the –OH group on the C5 of the 5’ base to the N3 at the 3’ base6,22 to form a transient zwitterion and then the oxygen atom attack of the C4 position at the 3’ base to form a transient oxetane-type structure (III). The transient H_2O formation model6,11, which proposes direct breakage of the C-O bond at the 5’ base after the initial PT, seems unlikely because it necessitates a series of PT reactions (including the protonation of the carbonyl group at the 3’ base), but there are no potential proton donors in proximity of this carbonyl group. In addition, any interruption in such a complicated scheme proposed by the H_2O model would be expected to give rise to damaged DNA at a significant rate, which is not observed in the repair reaction by (6-4) photolyase9,10. In contrast, our scheme, in which a simple transient oxetane formation facilitates the oxygen-atom transfer from the 5’ to 3’ base followed by C6-C4 bond split (IV), would be less prone to mutagenic side reaction, since after oxygen atom transfer and C-C bond cleavage the proton returns to the essential H364 residue and the electron returns to $FADH^{\bullet}$ to restore the enzyme to its active form and the 6-4PP to two thymine bases (V).

METHODS SUMMARY

Wild-type and mutant (6-4) photolyases were prepared as described previously23. The thymine-thymine 6-4PP substrate was prepared photochemically by UV (254 nm) irradiation of oligonucleotide d(GTATTATG) and purified by HPLC24. We used a 1-kHz femtosecond laser system to generate the 100-fs, 140-nJ pump pulse at a wavelength of 400 nm. The fluorescence transients were obtained by gating the emission with another 800-nm pulse. The transient absorptions were probed with the desired wavelengths generated from two

optical parametric amplifiers25,26. The instrument response times of the fluorescence and absorption detections are about 500 and 250 fs, respectively.

METHODS

(6-4) photolyase and 6-4PP substrate

The purification of *A. thaliana* (6-4) photolyase with an N-terminal His-tag has been described23. H364, a key amino acid for repair function, was mutated to polar N and Y, non-polar M and A, acidic D, and basic K for mutation studies. Mutant plasmids were constructed using QuickChange (Stratagene) based on the plasmid of wild-type enzyme. The mutated DNA was sequenced to ensure that no additional mutation was introduced. In femtosecond-resolved studies, the protein concentrations were 300 μM for fluorescence up-conversion, 200 μM for transient absorption in visible region and 50 μM in UV region. The reaction buffer at pH 7.5 contains 50 mM Tris-HCl, 100 mM NaCl, 1 mM EDTA, 5 mM dithiothreitol, and 50% (v/v) glycerol. The D_2O reaction buffer was prepared with 3 cycles of evaporating 1 mL reaction buffer to 0.5 mL and diluting it back to 1 mL by D_2O. Overall more than 80% H_2O in the reaction buffer was exchanged to D_2O. The 6-4PP substrate was prepared as reported24 with some modifications. Briefly, 5 mg d(GTATTATG) (synthesized by Integrated DNA Technologies) was dissolved in 10 mL water, put in a Petri dish at 4°C under argon in a sealed polyethylene pouch, and irradiated by two 254 nm germicidal lamps (General Electric, 15T8) at a 2 cm distance for 90 minutes. The 6-4PP was purified by HPLC, using a C18 reversed-phase column (Grace, 250mm×10mm) and a linear gradient of 8-9% (v/v) acetonitrile in 0.1 M triethylammonium acetate (pH 7.0) for 20 minutes at a flow rate of 4.5 mL/min. The 6-4PP was selectively collected by monitoring the absorbance at 260 nm and 325 nm. The final yield of 6-4PP is 0.5 mg, 10% of the starting material. The ratio of substrate to enzyme is 5:1 in all femtosecond-resolved studies.

Enzyme activity

Enzyme activity was measured as follows. A mixture of 1 μM enzyme with 50 μM 6-4PP in 200 μL reaction buffer at pH 7.5 (50 mM Tris-HCl, 100 mM NaCl, 10 mM dithiothreitol, 10% (v/v) glycerol) was prepared in a cuvette and then illuminated by two white-light lamps (General Electric, F15T8) with a distance of 6 cm at room temperature. A 20 μL reaction sample was removed every 30 minutes and was heated at 100 °C in dark for 10 minutes. The denatured protein was removed by centrifuge at 14,000 rpm for 10 minutes. The supernatant was loaded to HPLC and the repaired DNA was separated by a C18 reversed-phase column (Alltech, 250mm×4.6mm) with the same solvent as in 6-4PP's purification except with an 8-12% (v/v) gradient. The area of repaired 6-4PP is integrated by the 260 nm absorption curve along the retention time from HPLC. Along the illumination time the area increases linearly and the slope is proportional to the repair quantum yield of the enzyme activity. No repaired DNA was detected in substrate alone after white-light illumination. The absorption spectra of the enzyme activity (Fig. 3) were measured following a previously reported method23.

Femtosecond spectroscopy

All femtosecond-resolved measurements were carried out using the fluorescence up-conversion and transient absorption methods. The experimental layout has been detailed elsewhere25. Briefly, for femtosecond-resolved fluorescence detection, the pump wavelength at 400 nm was generated by the doubling of 800 nm in a 0.2 mm thick β-barium borate crystal (BBO, type I). The pump pulse energy typically was attenuated to 140-200 nJ before being focused into the sample cell. The resulting fluorescence from the sample was gated by another 800 nm beam in a 0.2 mm BBO crystal to obtain fluorescence transients at desired wavelengths. For transient absorption measurements, optical parametric amplifiers (OPA-800C and TOPAS, Spectra-Physics) were used to generate all desired probe wavelengths for different detection schemes. The spectral bandwidth is about 4 nm in UV region. The instrument response time is about 500 fs for fluorescence detection and about 250 fs for transient absorption measurements. All experiments were done at the magic angle (54.7°). Samples were keeping stirring during irradiation to avoid heating and photobleaching. All enzyme reactions in the femtosecond-resolved measurements were carried out under anaerobic conditions.

Supplementary Material

Refer to Web version on PubMed Central for supplementary material.

Acknowledgements

We thank Prof. Takeshi Todo and Prof. Teizo Kitagawa for the generous gift of *A. thaliana* (6-4) photolyase plasmid, Prof. Craig Forsyth for valuable discussions and Ya-Ting Kao and Dr. Chih-Wei Chang for help during the experiments. This work is supported in part by the National Institutes of Health (GM074813) and the Packard fellowship.

References

1. Mitchell DL. The relative cytotoxicity of (6-4) photoproduct and cyclobutane dimers in mammalian cells. Photochem. Photobiol. 1988; 48:51–57. [PubMed: 3217442]
2. Taylor JS. Unraveling the molecular pathway from sunlight to skin cancer. Acc. Chem. Res. 1994; 27:76–82.
3. Todo T, et al. A new photoreactivating enzyme that specifically repairs ultraviolet light-induced (6-4) photoproducts. Nature. 1993; 361:371–374. [PubMed: 8426655]
4. Sancar A. Structure and function of DNA photolyase and cryptochrome blue-light photoreceptors. Chem. Rev. 2003; 103:2203–2237. [PubMed: 12797829]
5. Hitomi K, et al. Functional motifs in the (6-4) photolyase crystal structure make a comparative framework for DNA repair photolyases and clock cryptochromes. Proc. Natl. Acad. Sci. U.S.A. 2009; 106:6962–6967. [PubMed: 19359474]
6. Maul MJ, et al. Crystal structure and mechanism of a DNA (6-4) photolyase. Angew. Chem. Int. Ed. Engl. 2008; 47:10076–10080. [PubMed: 18956392]
7. Kao Y-T, Saxena C, Wang L, Sancar A, Zhong D. Direct observation of thymine dimer repair in DNA by photolyase. Proc. Natl. Acad. Sci. U.S.A. 2005; 102:16128–16132. [PubMed: 16169906]
8. Zhong D. Ultrafast catalytic processes in enzymes. Curr. Opin. Chem. Biol. 2007; 11:174–181. [PubMed: 17353141]
9. Zhao XD, et al. Reaction mechanism of (6-4) photolyase. J. Biol. Chem. 1997; 272:32580–32590. [PubMed: 9405473]

10. Hitomi K, et al. Role of two histidines in the (6-4) photolyase reaction. J. Biol. Chem. 2001; 276:10103–10109. [PubMed: 11124949]
11. Glas AF, Schneider S, Maul MJ, Hennecke U, Carell T. Crystal structure of the T(6-4)C lesion in complex with a (6-4) DNA photolyase and repair of UV-induced (6-4) and dewar photolesions. Chem. Eur. J. 2009; 15:10387–10396. [PubMed: 19722240]
12. Joseph A, Prakash G, Falvey DE. Model studies of the (6-4) photoproduct photolyase enzyme: Laser flash photolysis experiments confirm radical ion intermediates in the sensitized repair of thymine oxetane adducts. J. Am. Chem. Soc. 2000; 122:11219–11225.
13. Berg OA, Eriksson LA, Durbeej B. Electron-transfer induced repair of 6-4 photoproducts in DNA: A computational study. J. Phys. Chem. A. 2007; 111:2351–2361. [PubMed: 17388321]
14. Yamamoto J, Hitomi K, Hayashi R, Getzoff ED, Iwai S. Role of the carbonyl group of the (6-4) photoproduct in the (6-4) photolyase reaction. Biochem. 2009; 48:9306–9312. [PubMed: 19715341]
15. Domratcheva T, Schlichting I. Electronic structure of (6-4) DNA photoproduct repair involving a non-oxetane pathway. J. Am. Chem. Soc. 2009; 131:17793–17799. [PubMed: 19921821]
16. Schleicher E, et al. Electron nuclear double resonance differentiates complementary roles for active site histidines in (6-4) photolyase. J. Biol. Chem. 2007; 282:4738–4747. [PubMed: 17164245]
17. Kao Y-T, Saxena C, Wang L, Sancar A, Zhong D. Femtochemistry in enzyme catalysis: DNA photolyase. Cell Biochem. Biophys. 2007; 48:32–44. [PubMed: 17703066]
18. Chang C-W, et al. Ultrafast solvation dynamics at binding and active sites of photolyases. Proc. Natl. Acad. Sci. U.S.A. 2010; 107:2914–2929. [PubMed: 20133751]
19. Wang H, et al. Protein dynamics control the kinetics of initial electron transfer in photosynthesis. Science. 2007; 316:747–750. [PubMed: 17478721]
20. Hitomi K, et al. Binding and catalytic properties of Xenopus (6-4) photolyase. J. Biol. Chem. 1997; 272:32591–32598. [PubMed: 9405474]
21. Marcus RA. R. A. Summarizing lecture: factors influencing enzymatic H-transfers, analysis of nuclear tunneling isotope effects and thermodynamic versus specific effects. Philos. T. R. Soc. B. 2006; 361:1445–1455.
22. Yamamoto J, Tanaka Y, Iwai S, et al. Spectroscopic analysis of the pyrimidine(6-4)pyrimidone photoproduct: insights into the (6-4) photolyase reaction. Org. Biomol. Chem. 2009; 7:161–166. [PubMed: 19081959]
23. Li J, Uchida T, Ohta T, Todo T, Kitagawa T. Characteristic structure and environment in FAD cofactor of (6-4) photolyase along function revealed by resonance Raman spectroscopy. J. Phys. Chem. B. 2006; 110:16724–16732. [PubMed: 16913812]
24. LeClerc JE, Borden A, Lawrence CW. The thymine-thymine pyrimidine-pyrimidone(6-4) ultraviolet light photoproduct is highly mutagenic and specifically induces 3' thymine-to-cytosine transitions in *Escherichia coli*. Proc. Natl. Acad. Sci. U.S.A. 1991; 88:9685–9689. [PubMed: 1946387]
25. Saxena C, Sancar A, Zhong D. Femtosecond dynamics of DNA photolyase: Energy transfer of antenna initiation and electron transfer of cofactor reduction. J. Phys. Chem. B. 2004; 108:18026–18033.
26. Kao Y-T, et al. Ultrafast dynamics and anionic active states of the flavin cofactor in cryptochrome and photolyase. J. Am. Chem. Soc. 2008; 130:7695–7701. [PubMed: 18500802]

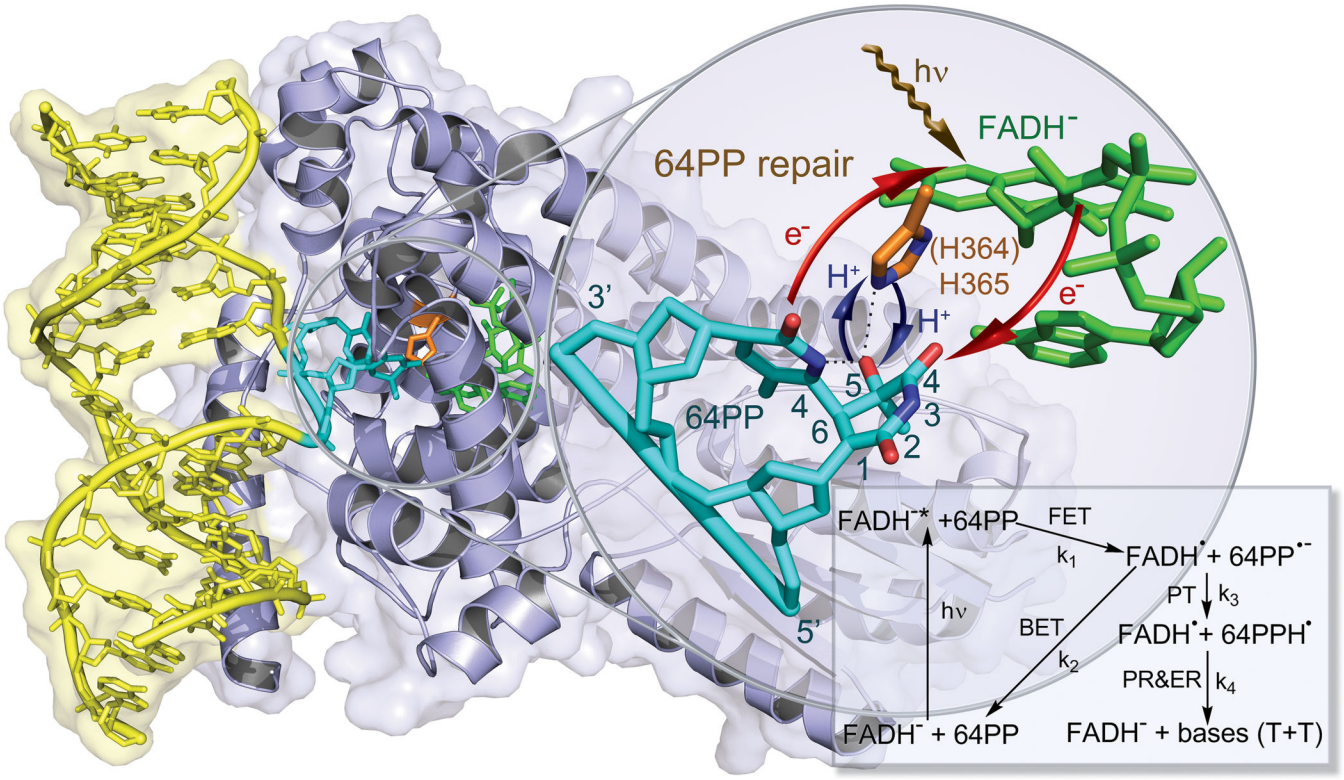

Figure 1. Enzyme-substrate complex structure and a possible repair scheme

X-ray structure of *D. melanogaster* (6-4) photolyase6 bound to DNA containing a (6-4) photoproduct. *A. thaliana* photolyase has a similar structure11 and conserved histidine residue in the active site (H364 in *A. thaliana* and H365 in *D. melanogaster*). The 6-4PP is flipped out of DNA and inserted into the active site. The close-up view shows the relative positions of the catalytic cofactor $FADH^-$, the conserved H364 (H365) residue, and the 6-4PP substrate with a proposed scheme for electron and proton transfers in the repair reaction. Shown in the repair scheme are forward electron transfer (FET) after light excitation, back electron transfer (BET) without repair, and the repair channel including initial proton transfer (PT) and late proton and electron return (PR and ER) after repair, with corresponding reaction rates (k_1-k_4) for the indicated steps.

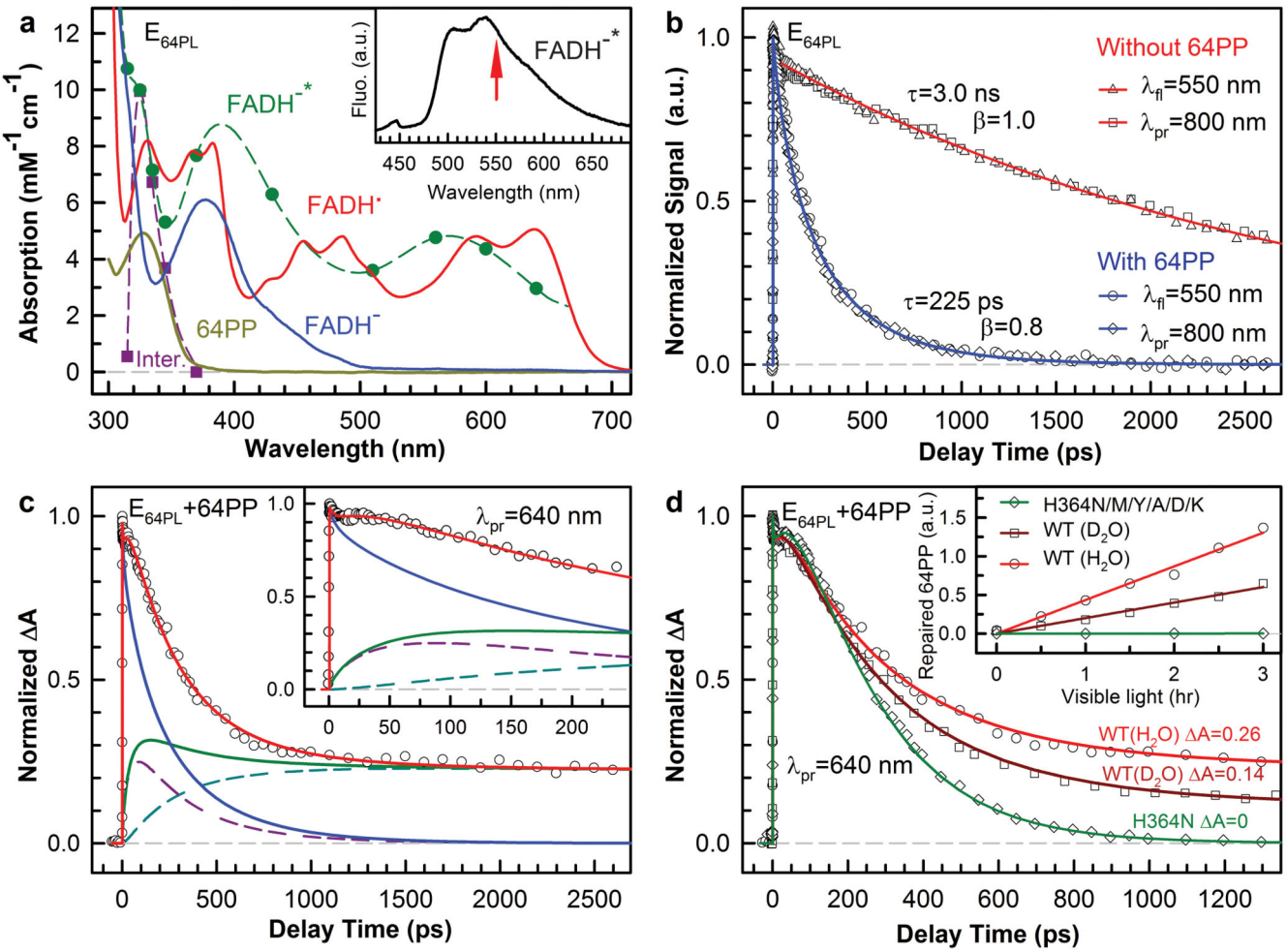

Figure 2. Femtosecond-resolved dynamics of flavin species involved in the damaged DNA repair

a. Absorption spectra and coefficients of purified protein with FADH•, converted active form $FADH^-$, damaged 6-4PP, and $FADH^{-*}$ determined by this study. Also determined is a 6-4PP-related reaction intermediate (Inter.) around 325 nm in Fig. 3. The fluorescence emission of $FADH^{-*}$ is shown in inset with an arrow indicating the gated wavelength. **b.** Normalized signals detected by both fluorescence (gated around the emission peak of 550 nm) and absorption (probed at 800 nm) methods with and without the substrate in the active site show the same lifetime and forward ET decays. The ET dynamics is best represented by a stretched-single-exponential decay. **c.** Transient absorption signal probed at 640 nm with both $FADH^{-*}$ (blue curve) and FADH• detection (green). The total FADH• signal is from the two contributions of the initially formed one (dashed purple; k_1 formation and k_2+k_3 decay in Fig. 1) and the branched one in the repair channel (dashed cyan; k_3 formation and k_4 decay). Note the flat signal in tens of picoseconds shown in inset, reflecting a fast apparent rise signal. **d.** Transient absorption signals probed at 640 nm of the H364N mutant and wild-type enzymes in D_2O compared with the wild-type in H_2O. The corresponding relative steady-state quantum yield measurements are shown in inset.

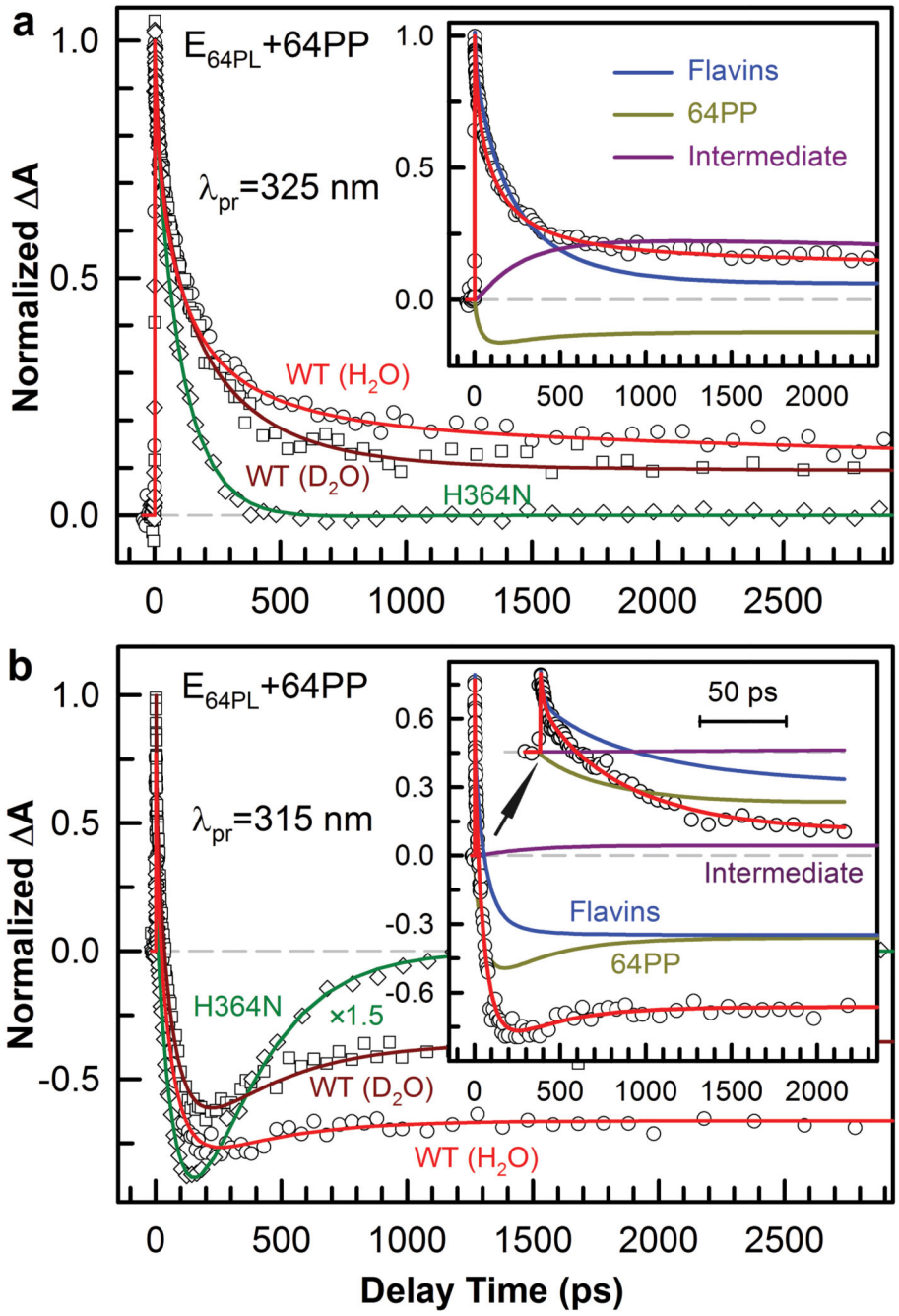

Figure 3. Femtosecond-resolved transient absorption dynamics of various species involved in the damaged DNA repair

Repair was probed at 325 nm (**a**) and 315 nm (**b**) for the H364N mutant and wild-type enzymes in D_2O and H_2O. The signals in the wild type include three contributions of overall flavin species ($FADH^-$, $FADH^{-*}$ and $FADH^{\bullet}$), 6-4PP and a captured intermediate shown in insets. The mutant signals decay to zero with a futile ET cycle. The determined absorption coefficients of $FADH^{-*}$ and the intermediate are shown in Fig. 2a.

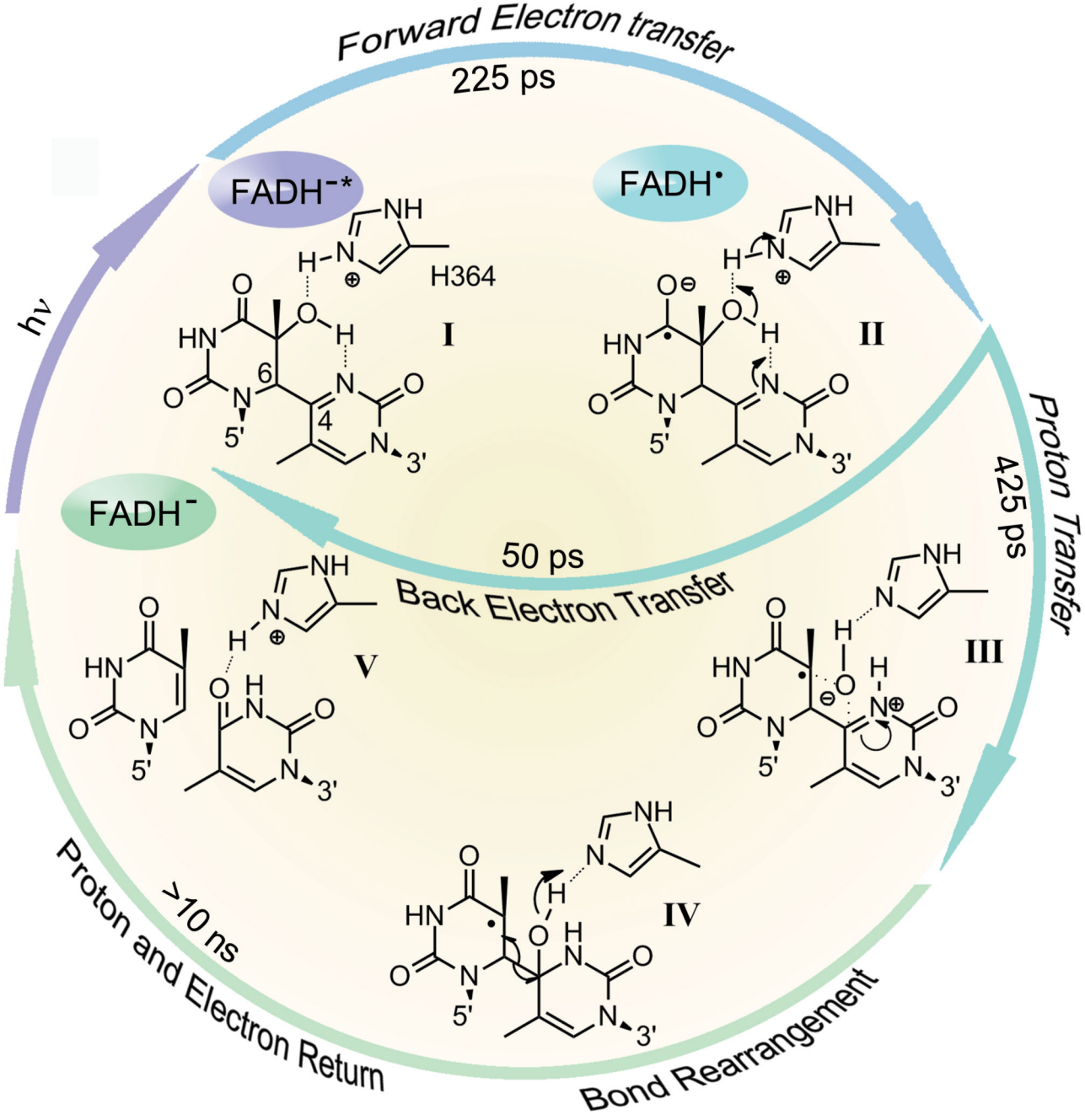

Figure 4. Repair photocycle of (6-4) thymine photoproduct by (6-4) photolyase

The resolved elementary steps include a forward electron transfer in 225 ps upon excitation, a back ET in 50 ps without any repair, and a parallel, catalytic PT between the enzyme (H364) and the substrate, induced by the initial electron transfer, in 425 ps. This PT is the determinant in repair and determines the overall repair quantum yield. The subsequent repair reactions involve a series of atom arrangements with bond braking and making and final

proton and electron returns (to H364 residue and flavin cofactor) to convert the 6-4PP to two thymine bases on time scales of longer than ten nanoseconds.